INTERNATIONAL JOURNAL OF INTEGRATED ENGINEERING
ISSN: 2229-838X e-ISSN: 2600-7916

IJIE

Vol. 16 No. 7 (2024) 124-134
https://publisher.uthm.edu.my/ojs/index.php/ijie

APTES Functionalization of cGNP Electrochemical Immunosensor for Detection of Immunoglobulin G

Mohd Azraie Mohd Azmi[1]*, Fatihatul Zuriati Makmon[1], Nur Azura Mohd Said[2], Hazana Razali[2], Mohd Ifwat Mohd Ghazali[3], Shahino Mah Abdullah[3], Owen J Guy[4]

[1] *Multidisciplinary Nanotechnology Centre Laboratory, Electronics Technology Section, British Malaysia Institute, Universiti Kuala Lumpur, Gombak, 53100, MALAYSIA*
[2] *Biotechnology & Nanotechnology Research Centre, MARDI, Serdang, 43400, MALAYSIA*
[3] *SMART-RG, Faculty of Science and Technology, Universiti Sains Islam Malaysia, Nilai, 71800, MALAYSIA*
[4] *Grove Building Extension, Swansea University, Singleton Park, SA2 8PP Swansea, WALES UNITED KINGDOM*

*Corresponding Author: mazraie@unikl.edu.my
DOI: https://doi.org/10.30880/ijie.2024.16.07.012

Article Info

Received: 25 June 2024
Accepted: 10 September 2024
Available online: 2 December 2024

Keywords

Graphene nanoplatelet, electrochemical immunosensor, APTES, immunoglobulin G, biosensor

Abstract

This paper demonstrates the development of carbon-based graphene nanoplatelet (cGNP) electrochemical immunosensor for the detection of immunoglobulin G (IgG). Initially, surface characterization via SEM revealed a smooth surface on the cGNP indicating successful GNP coverage using the drop-casting method. Screening of electrolyte buffers revealed that ferrocyanide and ferricyanide provided a favorable response with a current density of 9.369 µA. Functionalization of cGNP, was achieved using a 2% APTES solution during a 1-hour incubation period. Electrochemical characterization through cyclic voltammetry (CV) and electrochemical impedance spectroscopy (EIS) demonstrated excellent electrochemical activity when 0.1% bovine serum albumin (BSA) was employed as a blocking agent against 1 mg/ml IgG. Chronoamperometry (CA) confirmed IgG immobilization at a potential of 0.1 V. Notably, the immobilization of IgG resulted in an increase in the charge transfer resistance (R_{ct}) to 69.8 ± 2.3 Ω, attributed to the hindrance of biological molecules on interfacial electron transfer. Consequently, the proposed cGNP electrochemical immunosensor platform exhibited a robust analytical response, characterized by optimal antibody binding capacity. This superior performance can be attributed to the presence of GNP on the screen-printed carbon electrode (SPCE), which enhanced surface area, conductivity, and overall electrical properties. These attributes make this platform a promising candidate for further research in protein biomarker diagnosis and related applications.

1. Introduction

Electrochemical immunosensors have a rich history as one of the earliest transduction methods employed in biomedical applications for quantification and identification purposes. These sensors utilize inert materials such as gold, carbon, and platinum to enable sensitive, reliable, and rapid diagnostic capabilities [1]. Among these

materials, screen-printed carbon electrodes (SPCE) have emerged as highly promising platforms due to their advantages, including miniaturization, mass producibility, versatility, and the ability to design portable electrochemical immunosensors. However, despite their potential, SPCEs have been associated with limitations such as low electron transfer and reduced sensitivity, as noted in several studies [1-4]. Consequently, the integration of nanomaterials has opened new avenues for enhancing SPCE performance.

Nanomaterials, typically ranging from 1 to 100 nanometers in size, serve as intermediaries for improving electrical conductivity, connectivity, chemical accessibility, and biocompatibility in nanotechnology applications related to biomolecules [5]. Various well-known nanomaterials, including gold nanoparticles, carbon nanotubes (CNTs), conducting polymer nanotubes (CPNTs), and graphene, have found applications in biosensors [1, 2, 6, 7]. Graphene, a single layer of hexagonally arranged sp2 carbon atoms derived from graphite [8], possesses exceptional properties. It is characterized as a hydrophobic material stable in air up to 200°C, featuring a large surface area, ease of surface functionalization, high mechanical strength, and excellent electrical conductivity. Moreover, graphene exhibits promising applications in both in vitro and in vivo studies, potentially surpassing the utility of carbon nanotubes (CNTs) [1, 9].

In this paper, graphene nanoplatelets (GNP) were chosen as the nanomaterials for modifying SPCEs. GNP consists of short stacks of graphene sheets, typically comprising more than 30 graphene sheets, with thicknesses ranging from 5 to 10 nanometers and diameters spanning from 0.5 to 50 nanometers [10]. The platelet structure of GNP offers improved attachment during modification, primarily facilitated by Van der Waals forces along the (002) plane [11]. GNP exhibits high conductivity, efficient electron transfer, and a substantial surface area. However, it is essential to address GNP's inherent limitations, including a zero-band gap and inertness to reactions, which can hinder its competitiveness in certain applications. To overcome these challenges, surface modification with chemical functionalization was performed to enhance GNP's suitability for biosensing applications. Hence, Fig. 1 shows the schematic diagram of cGNP electrochemical immunosensor.

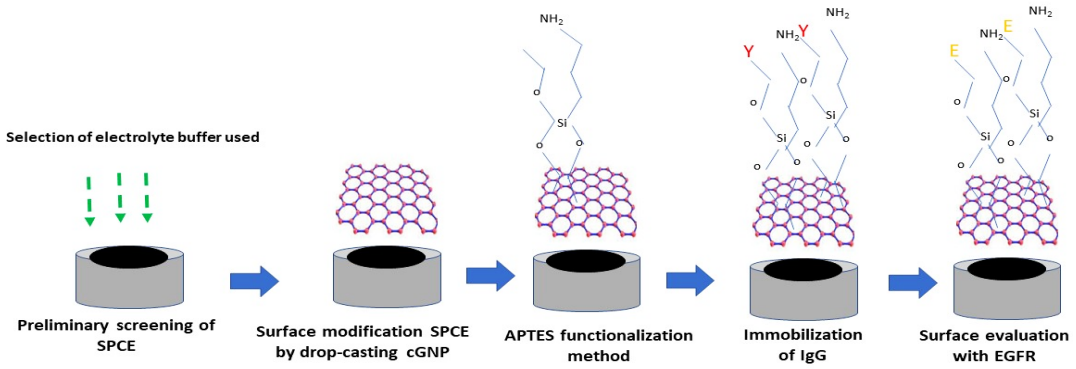

Fig. 1 *Schematic diagram of the cGNP electrochemical immunosensor (Y- antibody and E- EGFR)*

2. Materials, Chemicals and Buffer Preparations

Materials and reagents. The material for the substrate was selected as graphene nanoplatelet (GNP), which is produced using the electrochemical exfoliation method and was acquired from GO Advanced Sdn. Bhd. (1206920-P), Malaysia.

Electrodes. This study's electrochemical transducer is a three-electrode system 110 screen printed carbon electrode (110 SPCE) and was manufactured by Metrohm DropSens in Spain. The SPE comprises a carbon disc-shaped electrode with an area of 12.6 mm^2. Counter Electrode, included in the SPE configuration and Reference Electrode, utilizes a silver pseudo-reference electrode. These electrodes are screen-printed on a ceramic substrate with dimensions of 3.4 cm x 1.0 cm. A dielectric paste is a screen printed over the electrode system. This paste covers areas other than the three electrodes, leaving uncovered a specific area of 7 mm x 6 mm. The uncovered area serves as the electrochemical cell with a volume of 50 µL and the copper electric contacts are also present on the substrate [12]. In addition, SPCE has excellent properties, such as low background current, wide potential window, high chemical stability, and inexpensive techniques [13, 14]. The pre-experimental screening was conducted on the SPCE to identify the buffer analyte that will be used as a benchmark throughout this study using the cyclic voltammetry method.

Chemicals. Ferrocene carboxylic acid (FCA), potassium ferricyanide (K_3 [$Fe(CN)_6$]), potassium ferrocyanide (K_4 [$Fe(CN)_6$]), sodium chloride (KCl), phosphate buffered saline tablet (pH 7.4) (PBS), (3-Aminopropyl) triethoxysilane (APTES), 98% and sulphuric acid (H_2SO_4, 95%) were purchased from Sigma Aldrich, USA. Absolute ethanol (99%), acetone, and acetonitrile were supplied by Friendemann & Schmidt, USA. Bovine serum

Int. Journal of Integrated Engineering Vol. 16 No. 7 (2024) p. 124-134

albumin (BSA), N-(3-dimethylaminopropyl)-N′-ethylcarbodiimide hydrochloride (EDC), N-hydroxysuccinimide (NHS), alkaline phosphate conjugated goat affinity purified to rabbit immunoglobulin G (IG-AP), Tween 20, 3,3',5,5'-tetramethylbenzidine (TMB) were purchased from Sigma- Aldrich (St. Lois, MO, USA). All other chemicals and reagents are of analytical grade and were prepared using deionized (DI) water (18.2 M cm) from Mili-Q system (Millipore, USA).

Buffers and solutions preparations. The PBS solution was prepared by dissolving 1 tablet of PBS (Sigma Aldrich) into distilled water. The 0.1 M of potassium chloride (KCl) was prepared by weighing 1.86 g of KCl and dissolved into 250 mL of distilled water. The ferrocene carboxylic acid (FCA) in PBS was prepared by weighing 0.006 g of FCA and dissolved into 25 mL of PBS. The solution is then kept in an amber bottle. A 25 mL stock solution of 5 mM potassium hexacyanoferrate IV (K4 Fe $(CN)_6$) was prepared by dissolving 0.0528 g/mol/ L K_4 Fe $(CN)_6$ into 0.1 M KCl. A stock solution of 5 mM hexacyanoferricyanide III (K_3 Fe $(CN)_6$) was prepared by dissolving 1.6463 g/ mol/ L of K_3 Fe $(CN)_6$ into 25 mL of 0.1 M KCl. 2% APTES is prepared by diluting the concentration of APTES based on the equation below.

$$M_1V_1=M_2V_2 \quad (1)$$

M_1 stands for original concentrations and M_2 represents diluted concentrations, whereas V_1 represents original volume and V_2 represents diluted volume. In this study, functionalized modified GNP SPCE was linked to the antibody using EDC-NHS. A 400 mM stock solution of EDC and NHS is made for conjugation functionalized Ig G. In a nutshell, 0.153 g of EDC and 0.23 g of NHS were combined with 5 mL of deionized water and kept at -20 °C until needed.

2.1 Selection of Electrolyte Buffer

The selection of electrolyte buffer was important to select the right candidates for redox reaction. In this paper, ferrocene carboxylic acid (FCA) and ferrocyanide and ferricyanide (1:1) were compared to observe the electrochemical responses of the SPCE. CV is conducted at the potential window between 0.0 V to 0.7 V with a scan rate of 50 mVs-1 for three consecutive cycles. An ideal mediator would have an oxidation and reduction potential close to zero, which would eliminate the interference [15].

2.2 Surface Modification of SPCE

Briefly, 1 mg/ml of GNP powder was dispersed in a 0.1 M phosphate-buffered saline (PBS) solution. The dispersion is subjected to ultrasonication for one hour to ensure an even distribution of GNP in the solution. Next, 5 µL of the GNP in water solution is pipetted and dropped onto the working electrode of the SPCE. The GNP-modified SPCE is then dried in an oven for an hour. This process is repeated twice to achieve an even dispersion of GNP on the surface of the working electrode. After the drying process, the modified GNP SPCE is left to cool overnight at room temperature. This allows for complete adhesion of GNP to the SPCE surface. The modified GNP SPCE is gently rinsed with deionized water to remove any unbound materials on the working electrode. Hence, the GNP-modified SPCE is known as carbon-based graphene nanoplatelet (cGNP) (see results in section 3.2).

2.3 APTES Functionalization on cGNP

A method for functionalizing cGNP was achieved using the APTES (3-aminopropyltriethoxysilane) salinization method. This method involves activating the carboxyl functional group of the graphene-modified SPCE and adding an amide bond to it. This method was adapted from a previous work by Teixeira *et al.* [16], with minor modifications. The process starts with a graphene-modified SPCE that presumably has carboxyl functional groups on its surface. These carboxyl groups need to be activated, which might involve chemical treatment to make them more reactive. APTES is used to functionalize the electrode's surface. APTES contains an amino group (NH_2) that can form covalent bonds with carboxyl groups, leading to the formation of amide bonds. To determine the optimal conditions for this APTES functionalization, the concentration of APTES solution varied ranging from 1% to 4% v/v and salinization time from 30 minutes to 24 hours respectively. This optimization likely aimed to find the conditions that would yield the best functionalization results. Approximately 5 µL of the APTES solution was drop-casted onto the surface of the graphene-modified SPCE electrode. Drop-casting is a common method to deposit small volumes of a solution onto a substrate. After applying the APTES solution, the electrode was incubated at room temperature (RT). This incubation period allows the APTES molecules to react with the carboxyl groups on the electrode's surface and form amide bonds. After the incubation, the electrode surface was rinsed with distilled water. This step is likely done to remove any unreacted APTES and other impurities. Finally, the electrode was dried using nitrogen. Overall, this method is a common approach to functionalizing graphene-modified electrodes for various applications, particularly in electrochemistry and sensor development. The optimization study helps ensure that the functionalization process is efficient and can be tailored to specific research goals.

2.4 Immobilization of Immunoglobulin G

This paper focuses on the development of an immunosensor-based APTES functionalized on cGNP for the detection of serum rabbit immunoglobulin G (Ig G). To achieve this, optimizing the conditions for the immunosensor is essential. Furthermore, this step is crucial, as it forms the basis for the immunosensor's specificity and sensitivity. Optimization parameters require two key parameters, blocking properties and concentration of Ig G. Blocking properties vary the concentration of bovine serum albumin (BSA) at different levels (0.1%, 0.3%, 0.5%, 0.7%, and 1%) to determine the optimal blocking condition. BSA is often used to block non-specific binding sites and reduce background noise in immunoassays [17]. The concentration of Ig G varies from the concentration of Ig G in the samples at different levels (ranging from 0 to 0.1 mg/mL). This mimics the range of Ig G concentrations to detect in real-world samples. Optimization was recorded based on the changes in the current response. The measurement is carried out using a CA technique at a set potential of -0.1 V. CA is commonly used in electrochemical sensors to measure current changes in response to analyte binding. The collected data on current responses at various concentrations of BSA and Ig G will be analyzed to identify the optimal conditions for immunosensors. This analysis (BSA concentration) minimizes non-specific binding and optimizes the Ig G concentration for the best sensitivity and signal-to-noise ratio.

2.5 Characterizations

In this paper, two methods of characterization involved electrochemical and surface characterizations. The electrochemical characterization techniques used in this study were cyclic voltammetry (CV), chronoamperometry (CA) and electrochemical impedance spectroscopy (EIS). *Cyclic Voltammetry (CV)* was used to study reduction-oxidation (Redox) reactions, qualitatively and quantitatively. The working potential window used is between -0.3 V to 0.7 V at 50 mVs^{-1}. *Chronoamperometry (CA)* was used to study the kinetics of chemical reactions and diffusion process during immobilization of immunoglobulin G. A portable bipotentiostat/ galvanostat (Spain) with three electric contacts connector from DropSens were used to perform both CV and CA activities. Utilizing scanning electron microscopy (SEM), surface characterizations were conducted to evaluate the surface and binding of GNP and SPCE (see results at section 3.2). Electrochemical Impedance Spectroscopy (EIS) was performed using an Autolab PGSTAT30 from Eco, Chemie, Netherlands equipped with the Frequency Response Analyzer (FRA) module. A Faraday Cage containing a switch box was used to provide an interface to connect SPCE with the Autolab system. Impedance spectra were recorded in 0.1 M KCl solution containing 5 mM $K_3[Fe(CN)_6]$ + 5 mM $K_4[Fe(CN)_6$ (1:1) at room temperature with a fixed potential within a frequency range from 1 Hz to 10 MHz with a perturbation amplitude of 5 mV. The data acquisition and experiment control were done using Nova 1.10.1.9 software. The experimental setup is shown in Fig. 2.

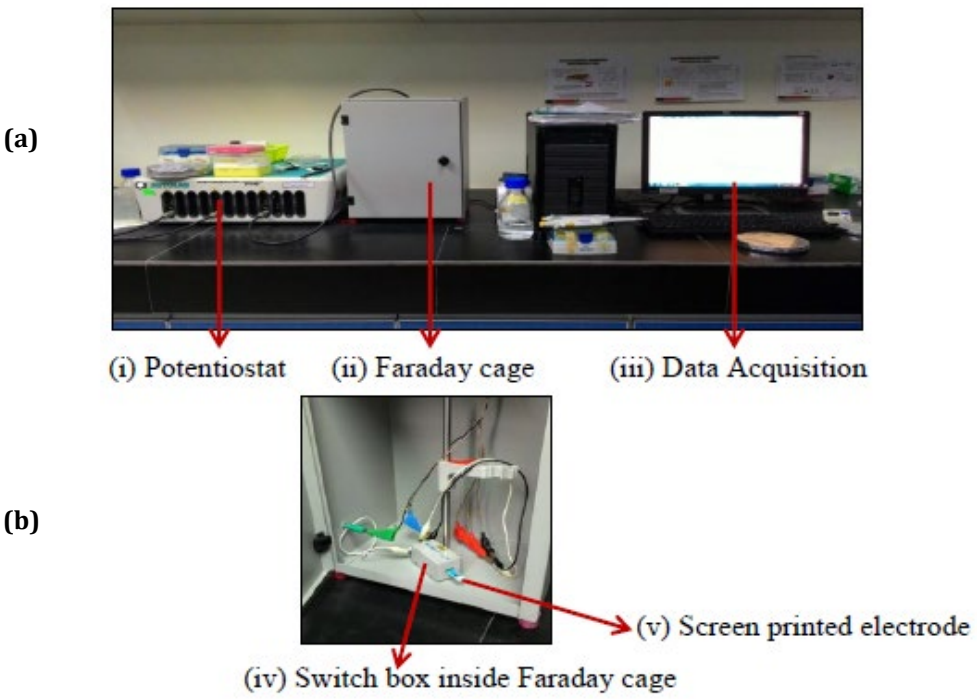

Fig. 2 *Electrochemical impedance spectroscopy instruments (a) Consist of potentiostat, faraday cage, and computer data acquisition; (b) Inside the Faraday cage consist of screen-printed electrode*

Int. Journal of Integrated Engineering Vol. 16 No. 7 (2024) p. 124-134

3. Results and Discussion

3.1 Comparison of Electrolyte Buffer

Buffer electrolyte is a mediator used to measure the electron transfer that occurs within the electrochemical system. An ideal mediator would have an oxidation and reduction potential close to zero, which would eliminate the interference [15]. Hence, in this paper, comparison studies between two electrolyte buffers were carried out between ferricyanide/ ferrocyanide in 0.1 M KCL and Ferrocene carboxylic acid (FCA) in PBS. Fig. 3 shows the CV comparison of ferricyanide/ ferrocyanide in 0.1 M KCl and FCA in PBS.

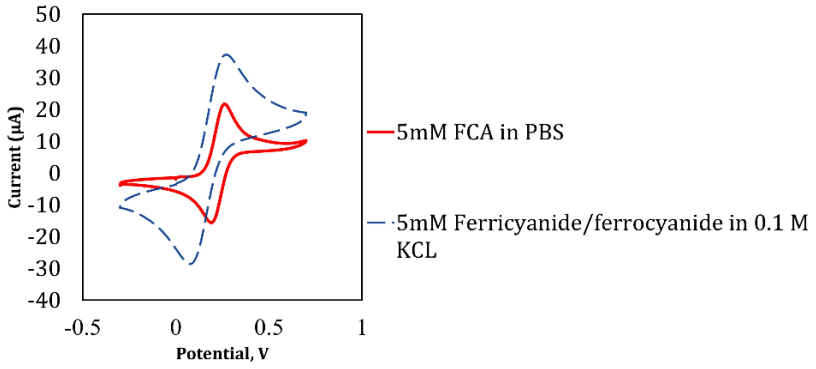

(a)

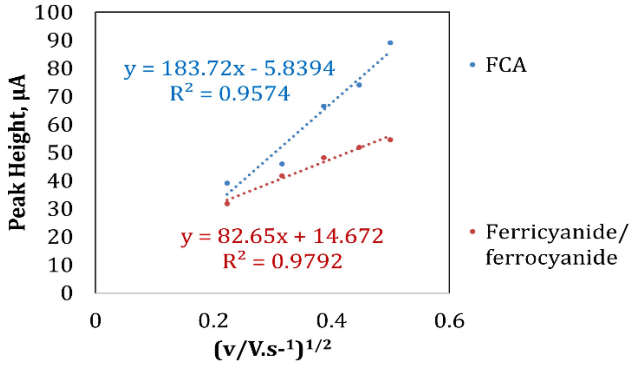

(b)

Fig. 3 *CV of SPCE in different Redox buffer electrolytes (a) 5 mM FCA in PBS (red line) and 5 mM Ferricyanide/ferrocyanide of 0.1 M KCl (orange line) at 50 mVs-1; (b) linear dependence of Ip and scan rate of both electrolyte buffer*

Both electrolyte buffers exhibit anodic and cathodic reactions due to the presence of ion charges, as shown in Fig. 2, Ferricyanide/ferrocyanide displayed more cathodic and anodic values compared to FCA. In contrast to FCA, a defined well-paired was observed in ferricyanide/ ferrocyanide. Ferricyanide and ferrocyanide (redox pairs) are composed of the ions $Fe(CN)_6^{3-}$ (ferricyanide) and $Fe(CN)_6^{4-}$ (ferrocyanide). These ions undergo reversible redox reactions, making them useful as electrolyte buffers. Butmee *et al.* discussed the choice of a redox electrolyte buffer for GNP (Gold Nanoparticle) immunosensor studies in their research. This choice of electrolyte buffer is a crucial aspect of designing and conducting experiments involving GNP immunosensors, as it can influence the performance and sensitivity of the sensor [18]. In addition, selecting the right electrolyte buffer is essential for achieving accurate and reliable results, as it can affect the stability of the sensor and the detection of target analytes.

CV was then quantitatively measured in the electron transfer-initiated chemical reactions. In this paper, CV is quantified into several parameters including peak potential separation (ΔE_p), peak ratio (I_p), and current density (J). The peak potential separation is measured to identify whether the CV process is either reversible, irreversible, or quasi-irreversible. A reversible process is determined as in Equation 2 and the values equal to 59.2/n at 25°C.

If the values of ΔE_p is more than 59.2/n mV, the CV is determined as quasi-reversible and vice-versa. In addition, the value of ΔE_p is increasing with increasing v.

$$Ep = Epc - Epa \tag{2}$$

Peak current ratio (I_{pa}) is used to calculate the chemical reaction of oxidation (O) and reduction (R) processes of CV cycles. The equilibrium of O and R can only be maintained during the CV experiment if both O and R are stable on the experimental time scale. This can be investigated based on the effect of V on the peak current ratio as described in Equation 3.

$$Ip = \frac{Ipa}{Ipc} \tag{3}$$

Current densities (J) refer to the amount of charge flowing through a specific cross-sectional area of a conductor, in this paper referring to the working electrode. The amount tends to remain constant in case of a steady charge flow. Nevertheless, the cross-sectional area of working electrodes differs in turn leads to varying density. However, in this paper the different buffer electrolyte effects on the current density when the working electrode remains the same is observed. Equation 3 displayed current density calculations. Table 1 summarizes the information gathered.

$$J = \frac{I}{A} \tag{4}$$

Table 1 *ΔEp, Ip ratio, and current densities electroactive area of FCA and ferricyanide/ ferrocyanide electrolyte buffer redox*

Electrolyte redox buffer	ΔEp, mV	Ip	Current densities
FCA	80	-1.0136	8.071
Ferricyanide/ ferrocyanide	81	1.2106	9.639

Table 1 shows the values of ΔEp, Ip ratio, and current densities for both electrolyte redox buffers. ΔEp values greater than 57 mV but less than 120 mV were nearly identical in both electrolytes' redox buffers. The current densities in both electrolyte redox buffers were nearly identical. The Ip ratio in FCA was less than one (-1.0136), whereas the Ip ratio in ferricyanide/ ferrocyanide was greater than one, indicating that ferricyanide/ ferrocyanide had better catalytic activity than FCA. This Ip ratio corresponds to the ferricyanide significance values with R2 shown in Fig. 2 (b) (0.9792). As a result, ferrocyanide/ ferricyanide exhibits a stable reaction that can be frequently used in the design of electrochemical immunosensors

3.2 Surface Characterization of GNP

Drop-casting is a popular method used in the modification of SPCE because it is inexpensive and convenient to apply in both laboratory and commercial applications. In this paper, GNP was used to improve the sensitivity and selectivity of the SPCE through the drop-casting method. The surface characterization was carried out initially to observe the changes on the surface of the SPCE before and after the modification. Fig. 4 shows the SEM morphologies of the bare SPCE and GNP modification SPCE by drop-casting. The morphology of SPCE is typical of graphite, with grains stacked in flakes (Fig. 4 (a)). A discernible heterogeneous distribution of submicron GNP sheets can be seen throughout the SPCE after GNP modification (Fig. 4 (b)). The wrinkled structure of GNP sheets may provide a larger active area for the functionalization process. Drop-casting revealed a smooth distribution of GNP in GNP-modified SPCE. In addition, the size of graphene is calculated and measured using Image J analysis software. Ferret diameter or max ferret is often used to represent the size of graphene flakes, indicating the maximum length across the flakes. In this study, the size of graphene flakes is larger than the carbon of a working screen-printed electrode with 3.96 μm. Hence, it provides the capabilities for better dispersion by drop-casting method to modify SPCE. The GNP-modified SPCE is known as cGNP.

Int. Journal of Integrated Engineering Vol. 16 No. 7 (2024) p. 124-134

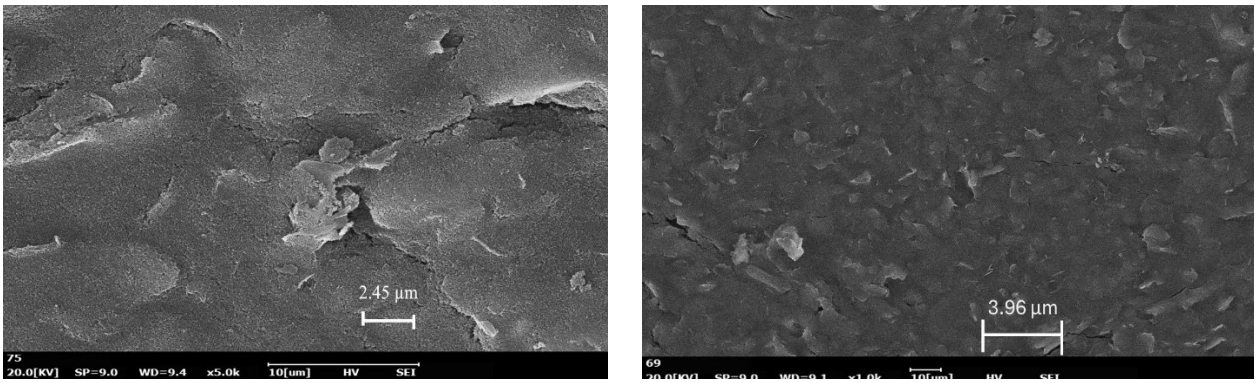

(a) (b)

Fig. 4 *Comparison of the SPCE's working electrode surface (a) before modification; (b) after GNP modification*

3.3 Optimal APTES Functionalization Condition for Immobilization of Immunoglobulin G

Functionalization was performed to create the ideal environment for IgG efficient immobilization. There are numerous silane compounds with different functional groups (amino, thiol, carboxyl, epoxide, etc.) accessible. Every functional group has unique characteristics. To effectively immobilize with IgG, APTES salinization was performed by optimizing its APTES concentration and incubation time. All other parameters are kept in their best possible condition during the optimization process. A series of APTES concentrations between 1% to 4% (v/v)) were carried out and were calculated for the values of total peak current response (ΔI_p) and charge transfer resistance (R_{ct}) as shown in Fig. 5 (a). The R_{ct} value was recorded from 23.06 Ω to 327.01 Ω suggesting that the resistance to the transfer of charge has significantly increased. This change could be due to various factors, such as changes in the electrode properties, the presence of inhibitors, or alterations in the electrochemical system's conditions. An increase in R_{ct} often indicates a decrease in the rate of charge transfer or electron transfer kinetics.

In contrast with ΔI_p value from 1.02 to 0.7 µA, respectively. A decrease in ΔIp suggests that there has been a reduction in the peak current difference between two specific electrochemical peaks. This change could be related to alterations in the electrochemical reaction kinetics or the presence of species that affect electron transfer at the electrode interface. These changes in R_{ct} and ΔIp values provide an important implication in electrochemical studies, comprehending how changes in experimental setups or the addition of various substances might impact charge transfer processes and peak current responses. A series of APTES incubation from 30 minutes to 24 hours were calculated for the values of total peak current response (ΔI_p) and charge resistance (R_{ct}) as shown in Fig. 5 (b). The time of incubation was measured to ensure the optimal aminated surface of cGNP. R_{ct} value was found to increase as incubation time increased from 1.10 Ω to 3.01 Ω in contrast with ΔIp value from 25.18 µA to 28.98 µA.

The highest R_{ct} was displayed by longer incubation times of 24 hours but showed a decrease in current value (Ip). During this period, the multilayer amino silane self-assembly may eventually accelerate, leading to an uneven distribution of the silane layer on the cGNP surface. [19-24].

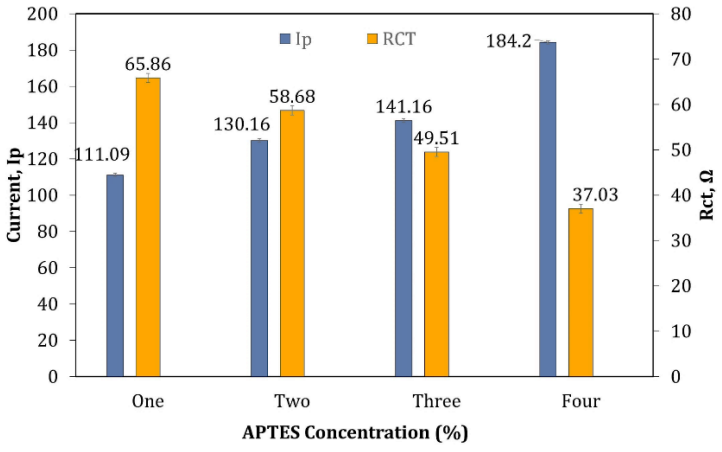

(a)

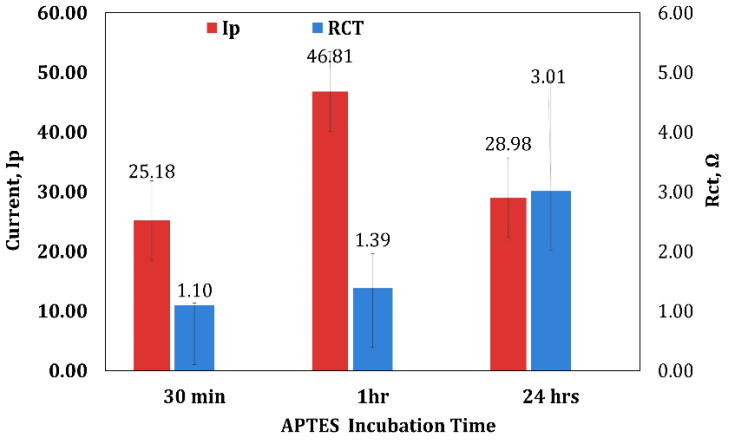

(b)

Fig. 5 *(a) Effect of different APTES concentrations at an hour APTES silanization time; (b) Effect of different incubation times at 2% concentration on the current response and resistance value of cGNP. Error bar represents standard deviation, n=3*

3.4 Optimization of BSA for Immobilization of Immunoglobulin G

BSA is an important protein that is used as a blocking agent in ELISA and immunosensor platforms. However, in certain circumstances, BSA could cause non-specific binding signals. Several studies have found that, BSA bound to human antibodies providing false-positive result [17]. To prevent this, a series of BSA standards was carried out by finding optimal concentration of BSA to use. In this paper, a series of 0%, 0.1%, 0.3%, and 0.5% of BSA concentration while maintaining the IgG concentration (1mg/mL) was conducted. Fig. 6 (a) showed the peak current (I_p) and R_{ct} of different BSA concentrations on immobilized rabbit IgG on the surface of salinization cGNP. The I_p value was found to have increased as increased in the BSA concentrations, 0.12 V to 22.37 V respectively.

Also, the R_{ct} values displayed an increase as concentration increased from 3.13 Ω to 103.91 Ω. Increased concentration of BSA leads to diminishment of IgG due to weak responses and also lead to an increase in non-specific bindings [17]. A stable reaction was found at 0.1% concentrations where both I_p and R_{ct} displayed similar values. Fig. 6 (b) shows a CA value to examine the sensitive activity of the varied BSA concentration at a set potential of -0.6 V to 0.6 V. Regardless of the BSA concentration, the excellent potential window is at 0.1 V. Hence, it was chosen as the potential CA value throughout this work due to its larger signal/background to its larger (S/B) ratio as compared to another potential window.

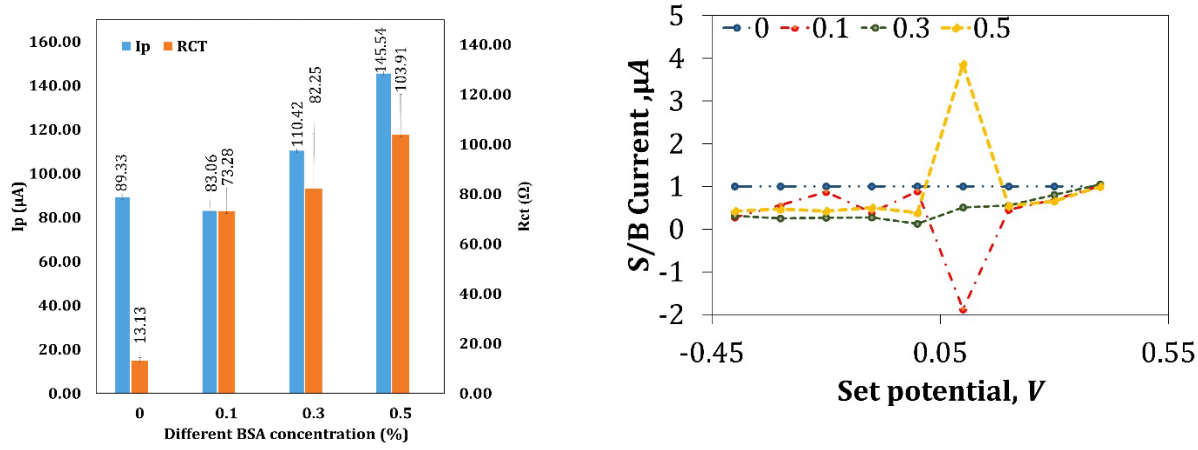

(a) **(b)**

Fig. 6 *Optimization of BSA (a) Ip and Rct; (b) CA signal/background plot potential window*

Int. Journal of Integrated Engineering Vol. 16 No. 7 (2024) p. 124-134

3.5 Electrochemical Characterization of cGNP Immunosensor

The electrochemical properties of the developed immunosensor were observed using CV and EIS in a solution comprising 5 mM ferricyanide and ferrocyanide in PBS at a pH of 7.4. A pair of clearly distinct redox peaks were seen in the CV obtained at SPCE (curve i) shown in Fig. 7 (a). A significant increase in peak current was observed at cGNP (curve ii). This indicates that graphene nanomaterial provides excellent electrical conductivity. Moreover, the large area displayed by the SEM image facilitates the electron transfer rate (see results Fig. 4(b)). As salinization by APTES on the cGNP surface, the peak current decreased due to the amino silane layer present on the cGNP surface (curve iii). The peak current was subsequently decreased because of the establishment of a bond between the antibody and the adsorbed APTES layer after IgG immobilization (curve iv).

EIS was carried out to further investigate the electron transfer resistance charge (R*ct*) on SPCE surface-modified electrodes (SPCE, cGNP, APTES, and IgG) shown in Fig. 7 (b). Surface modification of SPCE with GNP (drop cast, cGNP) decreases the R*ct* value from 1597.33 ± 1.53 Ω (curve i) to 1304.13 ± 12.23 Ω (curve ii). Deposition of APTES on the surface cGNP causes an increase in R*ct* with 12.46 ± 2.03 Ω (curve iii) indicating amino silane decreased the electron conduction pathway between the electrode and electrolyte [19]. Immobilizing with IgG increased the R*ct* value to 69.8 ± 2.3 Ω (curve iv) respectively, due to biological molecules retarded the interfacial electron transfer [16].

The results of the EIS being in good agreement with the results obtained from CV suggest that the development of the cGNP electrochemical immunosensor has been successful. EIS and CV are both electrochemical techniques used to study the behaviour of electrochemical systems. When the results of these two techniques agree, it indicates that the immunosensor is performing consistently and accurately. This consistency in results demonstrates that the sensor is reliable and capable of detecting the target analyte effectively.

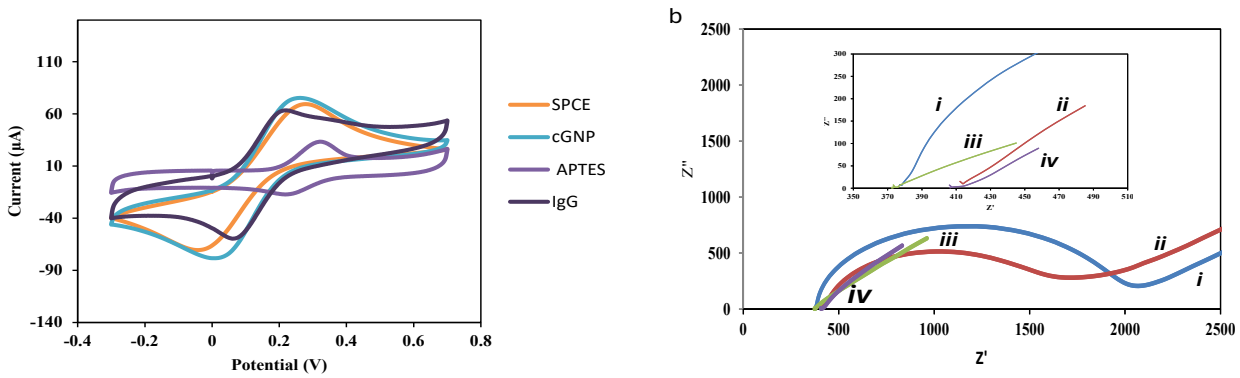

(a) **(b)**

Fig. 7 *Electrochemical characterization of cGNP immunosensor (a) CV; (b) EIS. Indication (i) control SPCE, (ii) cGNP, (iii) cGNP salinization with APTES, iv) further immobilization with IgG (cGNP+APTES+IgG)*

4. Conclusions

In conclusion, the observed decrease in peak current in CV can be attributed to the formation of a bond between the immobilized antibody and the adsorbed APTES layer, resulting in successful IgG immobilization on the cGNP-modified electrode. This immobilization of IgG led to a notable increase in the charge transfer resistance (R_{ct}) to a value of 69.8 ± 2.3 Ω, as confirmed by EIS. This increase was primarily due to the hindrance caused by biological molecules, which impeded interfacial electron transfer. The congruence of results obtained from both EIS and CV reinforces the notion that the electrochemical immunosensor has been well-designed and can fulfill its intended function effectively. The proposed cGNP electrochemical immunosensor platforms have exhibited a robust analytical response, particularly in terms of optimal antibody binding capacity. This enhanced performance can be attributed to the increased surface area, conductivity, and exceptional electrical properties conferred by the presence of GNP on the surface of SPCE. Additionally, the salinization with APTES has further improved the properties of GNP. These favorable characteristics make this platform a promising candidate for further research in the field of protein biomarker diagnosis and related applications. The successful integration of SPCE, GNP, APTES, and IgG immobilization has demonstrated the potential for developing sensitive and reliable point-of-care detection devices, with the capacity to contribute significantly to the advancement of diagnostic technologies

Acknowledgement

This study was supported by the Fundamental Research Grant Scheme, Ministry of Higher Education, Malaysia (FRGS 2016-1). We also extend our appreciation to Universiti Kuala Lumpur for their invaluable assistance and resources during the course of this research.

Conflict of Interest

Authors declare that there is no conflict of interests regarding the publication of the paper.

Author Contribution

The authors confirm contribution to the paper as follows: ***study conception and design:*** *Mohd Azraie Mohd Azmi, Fatihatul Zuriati Makmon, O.J. Guy;* ***data collection:*** *Fatihatul Zuriati Makmon, Hazana Razali;* ***analysis and interpretation of results:*** *Mohd Azraie Mohd Azmi, Fatihatul Zuriati Makmon, Nur Azura Mohd Said, Hazana Razali;* ***draft manuscript preparation:*** *All authors. All authors reviewed the results and approved the final version of the manuscript.*

References

[1] Raj M.A. and John S.A. (2019). Graphene-modified electrochemical sensors, in Graphene-Based Electrochemical Sensors for Biomolecules, ed: Elsevier, pp. 1-41. https://doi.org/10.1016/B978-0-12-815394-9.00001-7

[2] Badruzaman, N.A. (2022). Surface functionalization on graphene nanoplatelets using (3–aminopropyl)triethoxysilane for the detection of cyfra 21–1 biomarker, Master of Engineering Technology Thesis, Research and Innovation Centre, Universiti Kuala Lumpur British Malaysia Institute, Selangor.

[3] Jian, J. -M., Fu, L., Ji, J., Lin, L., Guo, X. and Ren, T. -L. (2018). Electrochemically reduced graphene oxide/gold nanoparticles composite modified screen-printed carbon electrode for effective electrocatalytic analysis of nitrite in foods, Sensors, and Actuators B: Chemical, vol. 262, pp. 125-136. https://doi.org/10.1016/j.snb.2018.01.164

[4] Chen, L., Tang, Y., Wang, K., Liu, C. and Luo, S. (2011). Direct electrodeposition of reduced graphene oxide on glassy carbon electrode and its electrochemical application, Electrochemistry communications, vol. 13, pp. 133-137. https://doi.org/10.1016/j.elecom.2010.11.033

[5] Azmi, M.A.M., Tehrani, Z., Lewis, R., Walker, K. -A., Jones, D., Daniels, D., Doak, S. and Guy O. (2014). Highly sensitive covalently functionalized integrated silicon nanowire biosensor devices for detection of cancer risk biomarkers, Biosensors and Bioelectronics, vol. 52, pp. 216-224. https://doi.org/10.1016/j.bios.2013.08.030

[6] Cruz-Pacheco, A.F., Monsalve, Y., Serrano-Rivero, Y., Salazar-Uribe, J., Moreno, E. and Orozco. J. (2023). Engineered synthetic nanobody-based biosensors for electrochemical detection of epidermal growth factor receptor, Chemical Engineering Journal, p. 142941, 2023. https://doi.org/10.1016/j.cej.2023.142941

[7] Makmon, F.Z.M., Azmi, M.A.M., Sabdin, S. ,Aziz, A. A. and Said, N.A. M. (2022). Electrochemical Activities of C/GNP Electrode for Ultrasensitive Immunosensors, in Advanced Materials and Engineering Technologies, ed: Springer, 2022, pp. 215-222. https://doi.org/10.1007/978-3-030-92964-0_21

[8] Novoselov, K., Geim, A., Morozov, S., Dubonos, S., Zhang, Y. and Jiang, D. (2004). Room-temperature electric field effect and carrier-type inversion in graphene films, *arXiv preprint cond-mat/0410631*. https://doi.org/10.48550/arXiv.cond-mat/0410631

[9] Tehrani, Z., Burwell, G. Azmi, M. A. M., Castaing, A. Rickman, R., Almarashi, J., Dunstan, P., Beigi, A.M., Doak, S. and Guy, O.(2014). Generic epitaxial graphene biosensors for ultrasensitive detection of cancer risk biomarker, 2D Materials, vol. 1, p. 025004. DOI 10.1088/2053-1583/1/2/025004

[10] Bianco, A., Cheng, H. -M., Enoki, T., Gogotsi, Y., Hurt, R.H., Koratkar, N., Kyotani, T., Monthioux, M., Park, C. R. and Tascon, J. M. (2013). All in the graphene family–A recommended nomenclature for two-dimensional carbon materials, vol. 65, ed: Elsevier, , pp. 1-6. https://doi.org/10.1016/j.carbon.2013.08.038.

[11] Zeng, Y., Bao, J., Zhao, Y., Huo, D., hen, M., Qi, Y., Yang, M., Fa, H., and Hou. C. (2018). A sandwich-type electrochemical immunoassay for ultrasensitive detection of non-small cell lung cancer biomarker CYFRA21-1, Bioelectrochemistry, vol. 120, pp. 183-189. https://doi.org/10.1016/j.bioelechem.2017.11.003

[12] Escamilla-Gómez, V., Hernández-Santos, D., González-García, M. B., Pingarrón-Carrazón, J. M. and Costa-García, A. (2009). Simultaneous detection of free and total prostate-specific antigen on a screen-printed electrochemical dual sensor, Biosensors and Bioelectronics, vol. 24, pp. 2678-2683. https://doi.org/10.1016/j.bios.2009.01.043

[13] Ferrari, A. G. -M., Rowley-Neale, S. J. and Banks, C.E. (2021). Screen-printed electrodes: Transitioning the laboratory in-to-the field, Talanta Open, vol. 3, p. 100032. https://doi.org/10.1016/j.talo.2021.100032

[14] Jiménez-Fiérrez, F., González-Sánchez, M.I., Jiménez-Pérez, R., Iniesta, J. and Valero, E. (2020). Glucose biosensor based on disposable activated carbon electrodes modified with platinum nanoparticles electrodeposited on poly (Azure A), Sensors, vol. 20, p. 448. https://doi.org/10.3390/s20164489
[15] P. Nicholas. (2020). Investigations Into the Design and Development of Novel Screenprinted Electrochemical Biosensors for Sugars, University of the West of England.
[16] Teixeira, S., Conlan, R.S., Guy, O. and Sales, M.G.F. (2014). Novel single-wall carbon nanotube screen-printed electrode as an immunosensor for human chorionic gonadotropin, Electrochimica Acta, vol. 136, pp. 323-329. https://doi.org/10.1016/j.electacta.2014.05.105
[17] Xiao, Y. and Isaacs S. N. (2012). Enzyme-linked immunosorbent assay (ELISA) and blocking with bovine serum albumin (BSA)—not all BSAs are alike, Journal of Immunological Methods, vol. 384, pp. 148-151, 2012. https://doi.org/10.1016/j.jim.2012.06.009
[18] P. Butmee, P., Tumcharern, G., Thouand, G., Kalcher, K. and Samphao, A. An ultrasensitive immunosensor based on manganese dioxide-graphene nanoplatelets and core-shell Fe3O4@ Au nanoparticles for label-free detection of carcinoembryonic antigen, Bioelectrochemistry, vol. 132, p. 107452. https://doi.org/10.1016/j.bioelechem.2019.107452
[19] Badruzaman, N.A.,Azmi, M.A.M and ,Mohd Said, N.A.M.(2020). Electrochemical Immunosensor Based on Highly Sensitive Amino Functionalized Graphene Nanoplatelets-Modified Screen Printed Carbon Electrode," in Key Engineering Materials, pp. 171-175. https://doi.org/10.4028/www.scientific.net/KEM.833.171
[20] Gunda, N.S.K.,Singh, M.,Norman, L., Kaur, K. and Mitra, S. K. (2014). Optimization and characterization of biomolecule immobilization on silicon substrates using (3-aminopropyl) triethoxysilane (APTES) and glutaraldehyde linker, Applied Surface Science, vol. 305, pp. 522-530. https://doi.org/10.4028/www.scientific.net/KEM.833.171
[21] Thakurta, S.G. and Subramanian, A. (2012). Fabrication of dense, uniform aminosilane monolayers: A platform for protein or ligand immobilization, Colloids and Surfaces A: Physicochemical and Engineering Aspects, vol. 414, pp. 384-392. https://doi.org/10.1016/j.colsurfa.2012.08.049
[22] Maniam, G., Sampe, J., Hamzah, A. A., & Faseehuddin, M. (2021, June). Biosensor Interface Controller for Chronic Kidney Disease Monitoring Using Internet of Things (IoT). In Journal of Physics: Conference Series (Vol. 1933, No. 1, p. 012110). IOP Publishing. DOI 10.1088/1742-6596/1933/1/012110
[23] Rabuan U, Mohd Nadzir MS, Abdullah Sham SZ, Izzati Wan Shaiful Bahri SB, Borah J, Majumdar S, Lei TM, Md Ali SH, A Wahab MI, Mohd Yunus NH. (2023). Evaluations of Low-cost Air Quality Sensors for Particulate Matter (PM 2.5) under Indoor and Outdoor Conditions. Sensors & Materials, 35. https://doi.org/10.18494/SAM4393
[24] Anuar, A. F. M., Yunus, N. H. M., Sampe, J., & Yunas, J. (2023, June). The development of wearable sensor for arcus pedis pressure assessment. In AIP Conference Proceedings (Vol. 2608, No. 1). AIP Publishing. https://doi.org/10.1063/5.0128017